Characterization of Nucleobase Analog FRET Acceptor tC_{nitro}

Søren Preus[†], *Karl Börjesson*[‡], *Kristine Kilså*[†], *Bo Albinsson*[‡] *and L. Marcus Wilhelmsson*[*,‡]

[†]Department of Chemistry, University of Copenhagen, Universitetsparken 5, DK-2100 Copenhagen, Denmark, [‡]Department of Chemical and Biological Engineering/Physical Chemistry, Chalmers University of Technology, S-41296 Gothenburg, Sweden

E-MAIL ADDRESS: marcus.wilhelmsson@chalmers.se

CORRESPONDING AUTHOR FOOTNOTE: L. Marcus Wilhelmsson: telephone number: +46 31 7723051 and fax number: +46 31 7723858.

Abstract

The fluorescent nucleobase analogs of the tricyclic cytosine (tC) family, tC and tC^O, possess high fluorescence quantum yields and single fluorescence lifetimes, even after incorporation into double-stranded DNA, which make these base analogs particularly useful as fluorescence resonance energy transfer (FRET) probes. Recently we reported the first all-nucleobase FRET pair consisting of tC^O as the donor and the novel tC_{nitro} as acceptor. The rigid and well-defined position of this FRET pair inside the DNA double helix, and consequently excellent control of the orientation factor in the FRET efficiency, are very promising features for future studies of nucleic acid structures. Here we provide the necessary spectroscopic and photophysical characterization of tC_{nitro} needed in order to utilize this probe as a FRET acceptor in nucleic acids. The lowest energy absorption band from 375-525 nm is shown to be the result of a single in-plane polarized electronic transition oriented ~27° from the molecular long axis. This band overlaps the emission bands of both tC and tC^O and the Förster characteristics of these donor-acceptor pairs are calculated for double-stranded DNA scenarios. In addition, the UV-Vis absorption of tC_{nitro} is monitored in a broad pH range and the neutral form is found to be totally predominant under physiological conditions with a pK_a of 11.1. The structure and electronic spectrum of tC_{nitro} is further characterized by density functional theory calculations.

Keywords: DNA base analog; photophysical properties; electronic transitions; pKa determination; molecular structure

Introduction

The development of synthetic nucleobase analogs continues to provide new tools for researchers working in the field of nucleic acids. Over the past 15 years artificial nucleobases have been developed to enhance duplex and triplex stability,[1-2] to detect single nucleotide polymorphisms (SNPs),[3-5] as electron spin labels,[6-7] and to gain insight into the function of DNA polymerases,[8] to name but a few. In particular, fluorescent nucleobase analogs have attracted wide attention as probes for nucleic acid structure, dynamics and interactions (for reviews see [9-13]). This specific class of probes includes 2-AP,[14-15] the pteridines 3MI and 6MI,[16-17] pyrrolo-C (PC),[18] the base discriminating fluorescent bases (BDF's) of Saito and co-workers,[11,19-21] the size-expanded (xDNA) nucleobases of Kool and co-workers,[22-23] and other more recently reported fluorescent base analogs.[24-33] Common for all the mentioned fluorescent base analogs are their sensitivity to the surrounding environment and most often a significant quenching of fluorescence in the base-stacking environment provided by double-stranded DNA. These features have been exploited in applications such as quencher free molecular beacons,[5] in monitoring or characterizing protein activity,[34-50] and in probing the local structure and dynamics of nucleic acids.[51-58] However, the low and unpredictable fluorescence quantum yields of these fluorophores in double-stranded DNA make them highly unsuitable for studies involving fluorescence resonance energy transfer (FRET).

The two fluorescent nucleobase analogs of the tricyclic cytosine family, 1,3-diaza-2-oxophenothiazine (tC) and 1,3-diaza-2-oxophenoxazine (tC^O), have previously been characterized and shown to work excellently as fluorescent probes in both single- and double-stranded DNA.[59-64] The high fluorescence quantum yields and single

fluorescence lifetimes, combined with a rigid and well-defined position inside the DNA double helix, make these base analogs particularly well suited for studies involving fluorescence anisotropy and FRET in nucleic acid containing systems.[65] Following this track, we recently demonstrated a novel FRET pair consisting of tC^O as the donor and the nitro-substituted 7-nitro-1,3-diaza-2-oxophenothiazine (tC_{nitro}, figure 1) as the acceptor.[66] The well-defined position and orientation of this FRET pair inside the DNA double helix is extraordinary and facilitates an unprecedentedly high control of the orientation factor in the FRET efficiency compared to other labeling strategies.[67-71] However, in order to utilize this FRET pair for structural studies of more complex systems the spectroscopical and photophysical properties of tC_{nitro} must be thoroughly characterized in terms of the number of transitions constituting the lowest energy absorption band, as well as the direction and magnitude of absorbing and emitting transition dipole moments.

Here we characterize the chromophoric properties of tC_{nitro} with special focus put on its use as an energy acceptor in FRET experiments. In particular we show that the lowest energy absorption band of tC_{nitro} is the result of a single electronic transition with an in-plane polarized transition dipole moment oriented ~27^o towards the NO_2-group from the molecular long-axis (figure 1b). In addition, the UV-Vis absorption spectrum of tC_{nitro} is monitored and shown to be preserved in a wide pH range. Furthermore, the molecular geometry of tC_{nitro} is optimized and electronic transitions are predicted using quantum chemical calculations.

Experimental methods

Synthesis. The tC_{nitro} nucleoside was prepared as described previously.[66] The potassium salt of 7-nitro-1,3-diaza-2-oxophenothiazine-3-yl acetic acid (KtC_{nitro}) (Figure 1b) was synthesized by saponification of the tertbutyl ester, which was obtained by alkylation of the anion of 7-nitro-1,3-diaza-2-oxophenothiazine[66] with tertbutylbromoacetate, following the general procedure of Eldrup *et al.*.[72]

Calculations. DFT geometry optimizations were performed in the ground state of the molecule using the B3LYP functional[73-75] and a 6-31G(d,p) basis set as implemented in the Gaussian 03 program package.[76] Restricted Hartree-Fock (RHF) wavefunctions were used. TDDFT[77-78] B3LYP/6-311+G(2d) calculations of the ten lowest energy excitations were performed using Gaussian 03. The amount of HOMO→LUMO character of the lowest energy electronic transition of the investigated compound was determined from the calculated CI-coefficients.

Linear dichroism. Linear dichroism (LD) is the difference in absorption of two mutually perpendicular planes of linearly polarized light, and was in this work exploited to estimate the direction of the transition dipole moment of tC_{nitro} aligned in a stretched polyvinyl alcohol (PVA) film.[79] The reduced LD of a uniaxial sample is defined as

$$\mathrm{LD^r} = \frac{A_{\parallel} - A_{\perp}}{A_{\mathrm{iso}}} = 3\frac{A_{\parallel} - A_{\perp}}{A_{\parallel} + 2A_{\perp}}$$

where $A_{\parallel}$ and $A_{\perp}$ are the absorption of light oriented parallel ($\parallel$) and perpendicular ($\perp$) to the macroscopic orientation axis (the direction of stretching) and A_{iso} is the absorbance of

the corresponding isotropic sample. The LD^r of a molecule with rod-like orientation is related to the angle, δ_i, between the *i*'th transition moment and the orientation axis by

$$LD^r = \frac{3}{2} S(\cos^2 \delta_i - 1)$$

where *S* is the Saupe orientation factor for the orientation axis. The LD measurements of tC_{nitro} in stretched PVA film were performed using a Varian Cary 4B spectrophotometer equipped with Glan air-space calcite polarizers in both sample and reference beam. The film was made from a 12.5% (w/w) aqueous solution of PVA that was prepared by dissolving PVA in water under heating to 85-95 ^oC and continuous stirring. 5 ml of the transparent PVA solution was mixed with 3 ml of an aqueous solution of the potassium salt of tC_{nitro} (~0.2 mg of substance). The mixture was poured onto rinsed horizontal glass plates and left to dry in a dust-free environment for a week. The film was then removed from the plates and mechanically stretched four times the original length under hot air from a hairdryer using a manually operated, in-house built device.

Fluorescence anisotropy. Fluorescence anisotropy, *r*, measurements were performed by exciting the sample using vertically polarized light and was calculated as the intensity ratio between the polarized and total emission emanating from the sample[80]

$$r = \frac{I_{\parallel} - GI_{\perp}}{I_{\parallel} + 2GI_{\perp}}$$

Here $I_{\parallel}$ and $I_{\perp}$ are the emission intensities measured through polarizers oriented parallel and perpendicular to the incident wave, respectively, and the *G*-factor is the ratio of the instrumental sensitivities for vertically and horizontally polarized light. For an immobile fluorophore, the angle between absorbing and emitting transition moments, α, is related to the fundamental anisotropy by

$$r_0 = \frac{1}{5}(3\cos^2\alpha - 1)$$

The fundamental fluorescence anisotropy of tC_{nitro} was measured by immobilizing the molecule in a propylene glycol (PG) glass at 200 K using an Oxford optistat DN cryostat and measure the excitation spectrum through Glan polarizers in both excitation and emission beam. Spectra were recorded on a Spex Fluorolog 3 spectrofluorimeter (JY Horiba) using excitations in the range 290-510 nm in 4 nm intervals with the emission monitored at 530 nm.

Magnetic circular dichroism. In magnetic circular dichroism (MCD) two CD spectra are recorded of the sample in the presence of a magnetic field oriented from north to south and south to north. The MCD spectrum is then calculated by subtracting the two[79,81]

$$2\mathrm{MCD}(\lambda) = \mathrm{NS}(\lambda) - \mathrm{SN}(\lambda)$$

where NS and SN represent the measured CD with the magnetic field oriented north-south and south-north, respectively. In the presence of an external magnetic field, two electronic transitions close in energy but with different polarizations will split into two

MCD signals of opposite sign resulting in a bisignate signal over the absorption band. Thus, MCD is a useful method to determine whether an absorption band contains one or several transitions. The MCD of tC_{nitro} was measured on a Jasco-J-720 CD spectropolarimeter equipped with a permanent horseshoe magnet. The MCD signal was recorded in the range 300-550 nm at a rate of 20 nm/min and the final spectrum was determined as an average of 8 acquisitions. A baseline of the solvent, a water:methanol (1:2) mixture, was used for both the NS and SN acquisitions. The concentration of the tC_{nitro} nucleoside was 240 μM.

UV-Vis absorption. UV-Vis absorption spectra were recorded on a Varian Cary 4000 spectrophotometer in 1 cm quartz cuvettes using pure solvent as baseline.

The pH titration of tC_{nitro} was performed by mixing a set of samples from aqueous stock solutions of tC_{nitro}, 2 M KOH and 1 M HCl producing 10-12 samples of equal tC_{nitro} concentrations but different pH values. The pH-range was tested from pH 0.2-12.2 and measured on a standard calibrated pH meter.

Singular value decomposition (SVD) is a mathematical tool with application in the deconvolution of spectra resulting from several absorbing species.[82] SVD analysis was performed using an in-house built Matlab script. The pH was rewritten into a vector of $[H^+]$ and used with a matrix containing the experimentally recorded spectra with each column representing a pH value and rows representing wavelengths. The pK_a was determined from the $[H^+]$ at which the ratio between the protonated and deprotonated components in the SVD analysis was 1.

Results and Discussion

Molecular geometry and electron distribution

The strict conditions set by the DNA double helix on a nucleobase analog in terms of H-bonding, base-stacking and steric hindrances make it highly relevant to determine the molecular geometry of tC_{nitro}. Two local energy minima on the potential energy surface of tC_{nitro} were identified from a B3LYP/6-31G(d,p) conformational search (figure 1. (a) chemical structure of the tricyclic cytosine analog tc_{nitro} and its base-pairing with guanine. the tricyclic expansion of natural cytosine is highlighted in red. also shown is the direction of major and minor groove when looking down the long axis of double stranded dna. (b) direction of the transition dipole moment, $\bar{\mu}$,, associated with the lowest energy electronic transition of tc_{nitro} ($\delta = 27^{o}$). for ktc_{nitro} r = $ch_2coo^{-}k^{+}$.

figure 2a). Calculations of the vibrational spectra confirmed that the optimized structures correspond to minima on the potential energy surface. As seen in figure 1. (a) chemical structure of the tricyclic cytosine analog tc_{nitro} and its base-pairing with guanine. the tricyclic expansion of natural cytosine is highlighted in red. also shown is the direction of major and minor groove when looking down the long axis of double stranded dna. (b) direction of the transition dipole moment, $\bar{\mu}$,, associated with the lowest energy electronic transition of tc_{nitro} ($\delta = 27^{o}$). for ktc_{nitro} r = $ch_2coo^{-}k^{+}$.

figure 2a, the two different geometries are the result of a distortion of the tricyclic framework symmetry due to the large sulphur atom present in the middle ring. The two local minima are mirror images corresponding to two geometries folded along the middle sulphur-nitrogen axis. This is also the result of AM1 calculations performed on the structurally similar tC base.[64] However, a slight distortion of the sulphur atom from the molecular plane is predicted by the DFT calculations compared to the AM1 optimized geometry. This is accompanied by a larger degree of bending (an angle of 26^{o} for the DFT optimized geometry compared to 18^{o} for AM1). The result that tC_{nitro} adopts a bent geometry is supported by the X-ray structure of the parent compound phenothiazine.[83-84]

The bend geometries of tC_{nitro} (and tC) do not affect the B-DNA secondary structure sterically since the expansion of these base analogs, compared to natural cytosine, is directed into the major groove of B-DNA. In addition, given the structural similarities between tC, tC^{O} and tC_{nitro}, as well as the fact that tC_{nitro} does not decrease duplex stability nor perturb the B-DNA structure in any significance,[66] we find it very likely that the base-flipping rate of tC_{nitro} is as slow as for tC and tC^{O}.[60-62] Furthermore, a very pronounced relationship between the DNA double helical structure and previously measured FRET efficiencies between tC^{O} and tC_{nitro} positioned inside double-stranded DNA supports the claim that tC_{nitro} is firmly stacked inside the DNA double helix.[66]

The two optimized frontier Kohn-Sham (KS) orbitals of tC_{nitro} are shown in figure 1. (a) chemical structure of the tricyclic cytosine analog tc_{nitro} and its base-pairing with guanine. the tricyclic expansion of natural cytosine is highlighted in red. also shown is the direction of major and minor groove when looking down the long axis of double

stranded dna. (b) direction of the transition dipole moment, $\vec{\mu}$,, associated with the lowest energy electronic transition of tc_{nitro} ($\delta = 27^{o}$). for ktc_{nitro} r = $ch_2coo^{-}k^{+}$.

figure 2b. The HOMO orbital is distributed almost throughout the entire molecular plane (although with low density at the nitro-group), while the LUMO orbital is mainly centered at the electron withdrawing nitro-group. As a result of the small spatial overlap of the HOMO and LUMO orbitals of tC_{nitro} the lowest energy electronic transition has a certain degree of charge-transfer character, which is a characteristic often seen for polycyclic nitroaromatics.[85-88]

Calculations of electronic transitions and frontier orbitals

The UV-Vis absorption spectrum of the nucleoside of tC_{nitro} in H_2O at 296 K is shown in figure 3a. The lowest energy absorption band is centered at 424 nm ($\varepsilon_{424\ nm}$ = 5400 $M^{-1}cm^{-1}$) but becomes slightly red shifted (10-15 nm) upon incorporation into DNA.[66] This Gaussian-shaped band is energetically well separated from higher energy absorption bands (ΔE ~1 eV).

The TDDFT B3LYP/6-311+G(2d) calculated electronic spectrum of the B3LYP/6-31G(d,p) optimized molecular geometry of tC_{nitro} is also depicted in figure 3a (vertical lines). In general, the overall appearance of the calculated spectrum agrees well with the experimentally recorded UV-Vis absorption spectrum in H_2O. The lowest energy absorption band of tC_{nitro} is found to be the result of a single electronic transition having 92% HOMO→LUMO character which is energetically well separated from higher

energy transitions (ΔE ~1 eV). The direction of the calculated transition dipole moment associated with the $S_0 \rightarrow S_1$ transition was predicted to be oriented in-plane and tilted 9^o towards the nitro-group from the molecular long-axis. The direction of the transition dipole moment of tC_{nitro} does not change when interconverting between the two bend geometries.

It is noted here, that the CT character of most of the excited states of tC_{nitro} (data not shown for transitions above the lowest in energy) results in slightly underestimated excitation energies, which is a well known problem when using local functionals, such as B3LYP, in the prediction of excitation energies of transitions involving KS orbitals of small spatial overlap.[89-91] The excitation energies shown in figure 3a have therefore been multiplied by a factor 1.08 to facilitate comparison with the overall spectral shape of the UV-Vis absorption spectrum of tC_{nitro} in H_2O.

Experimental characterization of the lowest energy absorption band

The electronic transition responsible for the lowest energy absorption band of tC_{nitro} was experimentally characterized using three different polarized optical spectroscopy techniques: fluorescence anisotropy, MCD, and LD. Figure 3b shows the fluorescence anisotropy of the nucleoside of tC_{nitro} immobilized in a PG glass at 200 K (red). The change from H_2O to PG does not change the shape of the absorption spectrum of the chromophore and only slightly shifts the absorption maximum of the lowest energy band to higher energy (5 nm; data not shown). As can be seen, the excitation anisotropy of tC_{nitro} almost reaches the theoretical maximum value of $r_A = 0.4$ over the lowest energy absorption band. First of all, this shows that the fluorophore is practically immobilized on the timescale of the excited state decay. Secondly, this value of r_A corresponds to

completely parallel absorbing and emitting transition dipole moments. Combined with the fact that r_A is essentially constant over the entire lowest energy absorption band, this indicates that the low energy absorption band of tC_{nitro} only contains a single electronic transition which, in turn, is the $S_0 \rightarrow S_1$ transition.

The MCD of the nucleoside of tC_{nitro} in a H_2O:methanol mixture (1:2) is shown in figure 3c. The use of a H_2O:methanol mixture as solvent was necessary in order to dissolve a sufficient amount of sample to detect the MCD signal. The change from pure H_2O to a H_2O:methanol mixture does not change the absorption spectrum of tC_{nitro} significantly (data not shown). As seen from figure 3c, the MCD signal over the region of the lowest absorption band of tC_{nitro} bears the same sign and appears as the mirror image of the absorption spectrum. Together with the fluorescence anisotropy measurement and the high level quantum chemical calculations (*vide supra*), this result strongly indicates that only a single electronic transition is responsible for the lowest energy absorption band of tC_{nitro}.

The direction of the $S_0 \rightarrow S_1$ transition dipole moment of tC_{nitro} was estimated based on the reduced linear dichroism of the potassium salt of tC_{nitro} (Figure 1b where R = $CH_2COO^-K^+$) aligned in a stretched polyvinyl alcohol (PVA) film (figure 3b, blue line). As can be seen, the LD^r of tC_{nitro} reaches a value of $LD^r = 1.62$ over the lowest energy absorption band. Assuming that tC_{nitro} orients similarly to the structurally comparable compound methylene blue within the PVA film (rod-like with a Saupe orientation factor of 0.78)[92] as previously assumed for tC and tC^O aligned in stretched PVA films,[61,64] the direction of the absorbing transition moment of tC_{nitro} is calculated to be tilted 27^o from the molecular long axis. The TDDFT calculations (*vide supra*) together with a FRET

study in double-stranded DNA[66] has shown that the tilt is towards the nitro-group. The fact that the LD^r is not constant over the entire absorption band of tC_{nitro} was also observed for the LD^r of tC and tC^O.[61,64] This feature may be the result of several absorbing species oriented differently in the film, such as aggregates of molecules formed due to the high sample concentration used in the film.

Emissive properties

The fluorescence quantum yield of tC_{nitro} is virtually zero, both in its monomeric form and after incorporation into single- and double-stranded DNA, but increases at temperatures below 225 K with an emission band centred at 530 nm in PG (data not shown). The weak or complete lack of fluorescence is a general property of nitroaromatic compounds and is usually either due to a fast intersystem crossing[88,93-95] or internal conversion[85,96] process. For tC_{nitro} we suggest that the quenching is due to an efficient S_1-S_0 internal conversion related to the charge transfer character of the first excited state. Studies addressing this are currently performed in our lab.

pH dependency

The pH range of the neutral form of tC_{nitro} was investigated by monitoring the UV-Vis absorption of tC_{nitro} at various pH values. The experiment shows that the neutral form of tC_{nitro} is predominant in a pH range from pH 11 down to at least pH 0.2 (the most acidic pH tested). The result of a pH 8-12 titration of the nucleoside of tC_{nitro} in H_2O is shown in figure 4a in which the arrows denote the spectral evolution as the pH increases. When increasing the pH, the low energy absorption band of tC_{nitro} at λ_{max} = 424 nm is replaced by a more intense band at λ_{max} = 500 nm corresponding to the deprotonated compound (deprotonation of the central enamine). The color of the sample correspondingly changes

from a clear yellow to a deep red color. The presence of several isosbestic points on the titration curves (at 227 nm, 253 nm, 306 nm, 387 nm and 436 nm) strongly indicates that only the protonated and deprotonated forms of tC_{nitro} are present in the solution.

Since the measured absorption spectrum of tC_{nitro}, at each of the different pH values, is a linear combination of the absorption spectra of the protonated and deprotonated species, the isolated absorption spectrum of each of the two components can successfully be deconvoluted using singular value decomposition. The isolated spectra obtained from the SVD analysis are shown in figure 4b. The overall isolated absorption spectrum of the deprotonated component is red-shifted compared to the neutral compound. This is most likely due to electrostatic interactions with the solvent resulting from the net negative charge of the deprotonated compound. The red-shift in wavenumbers is 3500 cm^{-1} for the lowest energy absorption band, and 2400 cm^{-1} for all the higher energy absorption maxima and the shoulder at 350 nm. This suggests that the energy of S_0 of tC_{nitro} is increased by 0.30 eV (2400 cm^{-1}) for the deprotonated anion, while the S_1 energy is stabilized by 0.14 eV (3500 - 2400 cm^{-1} = 1100 cm^{-1}), compared to the neutral protonated species in H_2O.

The pK_a of tC_{nitro} is calculated from the SVD analysis to be 11.1. This pK_a value of tC_{nitro} is 2 units lower than that found for tC (pK_a = 13.2),[64] most likely due to the electron-withdrawing NO_2-group that stabilizes the negative charge of the deprotonated compound.

Förster characteristics

The red-shifted absorption of tC_{nitro} has a considerable spectral overlap with the fluorescence spectra of both tC and tC^O. In table 1, we have summarized the calculated

overlap integrals[80] between the nucleobase analog FRET-pairs of the tricyclic cytosine family. Because the absorption and emission spectra, as well as the fluorescence quantum yields, of the nucleobase analogs change upon incorporation into DNA, the overlap integrals are also shown for the FRET-pairs positioned in double-stranded DNA. Furthermore, representative values of the critical Förster distances are shown in table 1 assuming $\kappa^2 = 2/3$ (freely rotating chromophores) and averaged donor quantum yields.[80] The overlap integrals between the absorption of monomeric tC_{nitro} and the emission of monomeric tC and tC^O are 4.7×10^{13} and 1.0×10^{14} $M^{-1}cm^{-1}nm^4$, respectively. The corresponding critical distances are 21.8 Å between monomeric tC-tC_{nitro} and 28.5 Å between tC^O-tC_{nitro}. Due to the red-shifted absorption of tC_{nitro} upon incorporation into DNA, the overlap integrals for FRET-pairs positioned in DNA are slightly larger compared to the monomeric FRET-pairs (5.4×10^{13} and 1.2×10^{14} $M^{-1}cm^{-1}nm^4$ for tC and tC^O as donors, respectively). Using the average quantum yields of tC and tC^O positioned in DNA, the corresponding critical distances become 23.4 Å for tC as donor and 27.2 Å for tC^O as donor. These values may be compared to the dimensions of the B-DNA double helix which has a length of approximately 34 Å per turn.

Since the Förster formulation is based on a point dipole approximation it is noted here that the FRET theory is not valid for close lying chromophores in which electronic couplings of other origins can be anticipated.[97] We have previously performed circular dichroism experiments on homodimers of tC as well as tC^O separated by 0-2 bases in DNA duplexes to examine the excitonic effect and found minor effects for the case where the homodimer is separated only by 0 bases (data not shown). The dipole-dipole resonance mechanism is therefore expected to be the totally predominant electronic

interaction between these base analogs in the distance range in which they operate (appr. 15-45 Å).

Conclusions and outlook

We have characterized the nucleobase analog tC_{nitro} with special focus put on its use as a FRET acceptor in nucleic acid studies. With a pK_a of 11.1 the neutral form of tC_{nitro} is totally predominant under physiological conditions. The lowest energy absorption band (375-525 nm) of this compound is the result of a single electronic transition well separated (~1 eV) from higher energy excitations and associated with an in-plane polarized transition dipole moment oriented ~27^o towards the nitro-group from the molecular long axis. A DFT conformational search performed at the B3LYP/6-31G(d,p) level identified two local minima on the potential energy surface of tC_{nitro} corresponding to two geometries folded along the middle sulphur-nitrogen axis, however, the direction of the transition dipole moment of tC_{nitro} is virtually the same within its two geometries.

Currently available FRET pairs for use in nucleic acid containing systems normally has longer Förster distances (>50 Å at κ^2 = 2/3) than the system presented here but lack high control of geometry and/or a stable quantum yield for the donor resulting in inaccuracies in estimating the Förster distance. This work, on the other hand, lays the foundation for future detailed structural studies of nucleic acid containing systems implementing tC_{nitro} as a FRET acceptor and tC or tC^O as the donor. The fact that these nucleobase donor-acceptor pairs can be rigidly positioned close to or inside the actual site of interest when studying nucleic acids opens up a number of new possibilities in the structural investigation of nucleic acids in solution. Since the energy transfer process is

highly dependent on both orientation and distance between the nucleobases, very detailed studies of nucleic acid structures and dynamics are in principle possible. Furthermore, through carefully designed experiments the nucleobase analog FRET pairs have the potential to thoroughly probe even subtle structural changes occurring in nucleic acids, *e.g.* resulting from the sequence specific interaction with other (bio)molecules or a change of physical chemical conditions.

Acknowledgments

This research is supported by the Swedish Research Council (VR) and the Danish Council for Independent Research | Natural Sciences (FNU).

References

(1) Herdewijn, P. *Antisense Nucleic Acid Drug Dev.* **2000**, *10*, 297.

(2) Wojciechowski, F.; Hudson, R. H. E. *Curr. Top. Med. Chem.* **2007**, *7*, 667.

(3) Wagenknecht, H. A. *Ann.NY Acad.Sci.* **2008**, *1130*, 122.

(4) Okamoto, A.; Tainaka, K.; Ochi, Y.; Kanatani, K.; Saito, I. *Mol. Biosyst.* **2006**, *2*, 122.

(5) Venkatesan, N.; Seo, Y. J.; Kim, B. H. *Chem. Soc. Rev.* **2008**, *37*, 648.

(6) Barhate, N.; Cekan, P.; Massey, A. P.; Sigurdsson, S. T. *Angew. Chem.-Int. Edit.* **2007**, *46*, 2655.

(7) Cekan, P.; Smith, A. L.; Barhate, N.; Robinson, B. H.; Sigurdsson, S. T. *Nucleic Acids Res.* **2008**, *36*, 5946.

(8) Jung, K. H.; Marx, A. *Cell. Mol. Life Sci.* **2005**, *62*, 2080.

(9) Asseline, U. *Curr. Org. Chem.* **2006**, *10*, 491.

(10) Hawkins, M. E. In *Topics in Fluorescence Spectroscopy: DNA Technology*; Lakowicz, J. R., Ed.; Kluwer Academic/Plenum Publishers: New York, 2003.

(11) Okamoto, A.; Saito, Y.; Saito, I. *J. Photochem. Photobiol. C-Photochem. Rev.* **2005**, *6*, 108.

(12) Rist, M. J.; Marino, J. P. *Curr. Org. Chem.* **2002**, *6*, 775.

(13) Wilson, J. N.; Kool, E. T. *Org. Biomol. Chem.* **2006**, *4*, 4265.

(14) Freese, E. *J. Mol. Biol.* **1959**, *1*, 87.

(15) Ward, D. C.; Reich, E.; Stryer, L. *J. Biol. Chem.* **1969**, *244*, 1228.

(16) Hawkins, M. E. *Cell Biochem. Biophys.* **2001**, *34*, 257.

(17) Hawkins, M. E. In *Fluorescence Spectroscopy*; Elsevier Academic Press Inc: San Diego, 2008; Vol. 450, p 201.

(18) Berry, D. A.; Jung, K. Y.; Wise, D. S.; Sercel, A. D.; Pearson, W. H.; Mackie, H.; Randolph, J. B.; Somers, R. L. *Tetrahedron Lett.* **2004**, *45*, 2457.

(19) Okamoto, A.; Tainaka, K.; Saito, I. *Tetrahedron Lett.* **2003**, *44*, 6871.

(20) Okamoto, A.; Tainaka, K.; Saito, I. *J. Am. Chem. Soc.* **2003**, *125*, 4972.

(21) Okamoto, A.; Tanaka, K.; Fukuta, T.; Saito, I. *J. Am. Chem. Soc.* **2003**, *125*, 9296.

(22) Krueger, A. T.; Lu, H. G.; Lee, A. H. F.; Kool, E. T. *Accounts Chem. Res.* **2007**, *40*, 141.

(23) Krueger, A. T.; Kool, E. T. *J. Am. Chem. Soc.* **2008**, *130*, 3989.

(24) Greco, N. J.; Sinkeldam, R. W.; Tor, Y. *Org. Lett.* **2009**, *11*, 1115.
(25) Mizuta, M.; Seio, K.; Miyata, K.; Sekine, M. *J. Org. Chem.* **2007**, *72*, 5046.
(26) Srivatsan, S. G.; Weizman, H.; Tor, Y. *Org. Biomol. Chem.* **2008**, *6*, 1334.
(27) Butler, R. S.; Cohn, P.; Tenzel, P.; Abboud, K. A.; Castellano, R. K. *J. Am. Chem. Soc.* **2009**, *131*, 623.
(28) Dyrager, C.; Börjesson, K.; Diner, P.; Elf, A.; Albinsson, B.; Wilhelmsson, L. M.; Grøtli, M. *Eur. J. Org. Chem.* **2009**, 1515.
(29) Mizuta, M.; Seio, K.; Ohkubo, A.; Sekine, M. *J. Phys. Chem. B* **2009**, *113*, 9562.
(30) Miyata, K.; Mineo, R.; Tamamushi, R.; Mizuta, M.; Ohkubo, A.; Taguchi, H.; Seio, K.; Santa, T.; Sekine, M. *J. Org. Chem.* **2007**, *72*, 102.
(31) Miyata, K.; Tamamushi, R.; Ohkubo, A.; Taguchi, H.; Seio, K.; Santa, T.; Sekine, M. *Org. Lett.* **2006**, *8*, 1545.
(32) Greco, N. J.; Tor, Y. *J. Am. Chem. Soc.* **2005**, *127*, 10784.
(33) Wojciechowski, F.; Hudson, R. H. E. *J. Am. Chem. Soc.* **2008**, *130*, 12574.
(34) Hariharan, C.; Reha-Krantz, L. J. *Biochemistry* **2005**, *44*, 15674.
(35) Wojtuszewski, K.; Hawkins, M. E.; Cole, J. L.; Mukerji, I. *Biochemistry* **2001**, *40*, 2588.
(36) Allan, B. W.; Beechem, J. M.; Lindstrom, W. M.; Reich, N. O. *J. Biol. Chem.* **1998**, *273*, 2368.
(37) Frey, M. W.; Sowers, L. C.; Millar, D. P.; Benkovic, S. J. *Biochemistry* **1995**, *34*, 9185.
(38) Srivatsan, S. G.; Greco, N. J.; Tor, Y. *Angew. Chem.-Int. Edit.* **2008**, *47*, 6661.
(39) Raney, K. D.; Sowers, L. C.; Millar, D. P.; Benkovic, S. J. *Proc. Natl. Acad. Sci. U. S. A.* **1994**, *91*, 6644.
(40) Hochstrasser, R. A.; Carver, T. E.; Sowers, L. C.; Millar, D. P. *Biochemistry* **1994**, *33*, 11971.
(41) Jia, Y. P.; Kumar, A.; Patel, S. S. *J. Biol. Chem.* **1996**, *271*, 30451.
(42) Ujvari, A.; Martin, C. T. *Biochemistry* **1996**, *35*, 14574.
(43) Zhong, X. J.; Patel, S. S.; Werneburg, B. G.; Tsai, M. D. *Biochemistry* **1997**, *36*, 11891.
(44) Holz, B.; Klimasauskas, S.; Serva, S.; Weinhold, E. *Nucleic Acids Res.* **1998**, *26*, 1076.
(45) Allan, B. W.; Reich, N. O.; Beechem, J. M. *Biochemistry* **1999**, *38*, 5308.
(46) Allan, B. W.; Reich, N. O. *Biochemistry* **1996**, *35*, 14757.
(47) Stivers, J. T.; Pankiewicz, K. W.; Watanabe, K. A. *Biochemistry* **1999**, *38*, 952.
(48) Liu, C. H.; Martin, C. T. *J. Biol. Chem.* **2002**, *277*, 2725.

(49) Hariharan, C.; Bloom, L. B.; Helquist, S. A.; Kool, E. T.; Reha-Krantz, L. J. *Biochemistry* **2006**, *45*, 2836.
(50) Liu, C. H.; Martin, C. T. *J. Mol. Biol.* **2001**, *308*, 465.
(51) Menger, M.; Eckstein, F.; Porschke, D. *Biochemistry* **2000**, *39*, 4500.
(52) Guest, C. R.; Hochstrasser, R. A.; Sowers, L. C.; Millar, D. P. *Biochemistry* **1991**, *30*, 3271.
(53) Xu, D. G.; Evans, K. O.; Nordlund, T. M. *Biochemistry* **1994**, *33*, 9592.
(54) Ramreddy, T.; Kombrabail, M.; Krishnamoorthy, G.; Rao, B. J. *J. Phys. Chem. B* **2009**, *113*, 6840.
(55) Jean, J. M.; Hall, K. B. *Biochemistry* **2004**, *43*, 10277.
(56) Ramreddy, T.; Rao, B. J.; Krishnamoorthy, G. *J. Phys. Chem. B* **2007**, *111*, 5757.
(57) Larsen, O. F. A.; van Stokkum, I. H. M.; Gobets, B.; van Grondelle, R.; van Amerongen, H. *Biophys. J.* **2001**, *81*, 1115.
(58) Dash, C.; Rausch, J. W.; Le Grice, S. F. J. *Nucleic Acids Res.* **2004**, *32*, 1539.
(59) Börjesson, K.; Sandin, P.; Wilhelmsson, L. M. *Biophys. Chem.* **2009**, *139*, 24.
(60) Engman, K. C.; Sandin, P.; Osborne, S.; Brown, T.; Billeter, M.; Lincoln, P.; Nordén, B.; Albinsson, B.; Wilhelmsson, L. M. *Nucleic Acids Res.* **2004**, *32*, 5087.
(61) Sandin, P.; Börjesson, K.; Li, H.; Mårtensson, J.; Brown, T.; Wilhelmsson, L. M.; Albinsson, B. *Nucleic Acids Res.* **2008**, *36*, 157.
(62) Sandin, P.; Wilhelmsson, L. M.; Lincoln, P.; Powers, V. E. C.; Brown, T.; Albinsson, B. *Nucleic Acids Res.* **2005**, *33*, 5019.
(63) Wilhelmsson, L. M.; Holmén, A.; Lincoln, P.; Nielson, P. E.; Nordén, B. *J. Am. Chem. Soc.* **2001**, *123*, 2434.
(64) Wilhelmsson, L. M.; Sandin, P.; Holmén, A.; Albinsson, B.; Lincoln, P.; Nordén, B. *J. Phys. Chem. B* **2003**, *107*, 9094.
(65) Stengel, G.; Gill, J. P.; Sandin, P.; Wilhelmsson, L. M.; Albinsson, B.; Nordén, B.; Millar, D. *Biochemistry* **2007**, *46*, 12289.
(66) Börjesson, K.; Preus, S.; El-Sagheer, A. H.; Brown, T.; Albinsson, B.; Wilhelmsson, L. M. *J. Am. Chem. Soc.* **2009**, *131*, 4288.
(67) Clegg, R. M.; Murchie, A. I. H.; Zechel, A.; Lilley, D. M. J. *Proc. Natl. Acad. Sci. U. S. A.* **1993**, *90*, 2994.
(68) Hurley, D. J.; Tor, Y. *J. Am. Chem. Soc.* **2002**, *124*, 13231.
(69) Iqbal, A.; Arslan, S.; Okumus, B.; Wilson, T. J.; Giraud, G.; Norman, D. G.; Ha, T.; Lilley, D. M. J. *Proc. Natl. Acad. Sci. U. S. A.* **2008**, *105*, 11176.
(70) Lewis, F. D.; Zhang, L. G.; Zuo, X. B. *J. Am. Chem. Soc.* **2005**, *127*, 10002.
(71) Sapsford, K. E.; Berti, L.; Medintz, I. L. *Angew. Chem.-Int. Edit.* **2006**, *45*, 4562.
(72) Eldrup, A. B.; Nielsen, B. B.; Haaima, G.; Rasmussen, H.; Kastrup, J. S.; Christensen, C.; Nielsen, P. E. *Eur. J. Org. Chem.* **2001**, 1781.

(73) Becke, A. D. *J. Chem. Phys.* **1993**, *98*, 5648.
(74) Lee, C. T.; Yang, W. T.; Parr, R. G. *Phys. Rev. B* **1988**, *37*, 785.
(75) Stephens, P. J.; Devlin, F. J.; Chabalowski, C. F.; Frisch, M. J. *J. Phys. Chem.* **1994**, *98*, 11623.
(76) Frisch, M. J. *e. a.*; Gaussian, Inc.: Wallington Ford CT, 2004.
(77) Marques, M. A. L.; Gross, E. K. U. *Annu. Rev. Phys. Chem.* **2004**, *55*, 427.
(78) Burke, K.; Werschnik, J.; Gross, E. K. U. *J. Chem. Phys.* **2005**, *123*.
(79) Rodger, A.; Nordén, B. *Circular Dichroism and Linear Dichroism*; Oxford University Press, 1997.
(80) Lakowicz, J. R. *Principles of Fluorescence Spectroscopy*; 3rd ed.; Springer: New York, 2006; Vol. 3rd.
(81) Mason, W. M. *Magnetic Circular Dichroism*; John Wiley & Sons: New Jersey, 2007.
(82) Hendler, R. W.; Shrager, R. I. *J. Biochem. Biophys. Methods* **1994**, *28*, 1.
(83) Bell, J. D.; Blount, J. F.; Briscoe, O. V.; Freeman, H. C. *Chem. Commun.* **1968**, 1656.
(84) McDowell, J. J. H. *Acta Crystallogr. B* **1976**, *32*, 5.
(85) Mohammed, O. F.; Vauthey, E. *J. Phys. Chem. A* **2008**, *112*, 3823.
(86) Khalil, O. S.; Bach, H. G.; McGlynn, S. P. *J. Mol. Spectrosc.* **1970**, *35*, 455.
(87) Mikula, J. J.; Stuebing, E. W.; Anderson, R. W.; Harris, L. E. *J. Mol. Spectrosc.* **1972**, *42*, 350.
(88) Zugazagoitia, J. S.; Almora-Diaz, C. X.; Peon, J. *J. Phys. Chem. A* **2008**, *112*, 358.
(89) Dreuw, A.; Head-Gordon, M. *J. Am. Chem. Soc.* **2004**, *126*, 4007.
(90) Dreuw, A.; Weisman, J. L.; Head-Gordon, M. *J. Chem. Phys.* **2003**, *119*, 2943.
(91) Tozer, D. J. *J. Chem. Phys.* **2003**, *119*, 12697.
(92) Nordén, B. *J. Chem. Phys.* **1980**, *72*, 5032.
(93) Ohtani, H.; Kobayashi, T.; Suzuki, K.; Nagakura, S. *Bull. Chem. Soc. Jpn.* **1980**, *53*, 43.
(94) Morales-Cueto, R.; Esquivelzeta-Rabell, M.; Saucedo-Zugazagoitia, J.; Peon, J. *J. Phys. Chem. A* **2007**, *111*, 552.
(95) Takezaki, M.; Hirota, N.; Terazima, M. *J. Phys. Chem. A* **1997**, *101*, 3443.
(96) Kovalenko, S. A.; Schanz, R.; Farztdinov, V. M.; Hennig, H.; Ernsting, N. P. *Chem. Phys. Lett.* **2000**, *323*, 312.
(97) Beljonne, D.; Curutchet, C.; Scholes, G. D.; Silbey, R. J. *J. Phys. Chem. B* **2009**, *113*, 6583.

Table 1. Calculated overlap integrals and critical Förster distances (for $\kappa^2 = 2/3$) of the tC-tC_{nitro} and tC^O-tC_{nitro} nucleobase analog donor-acceptor pairs.

Donor	Φ_f	n^a	J /$M^{-1}cm^{-1}nm^4$	R_0 /Å
Monomer[b]*:*				
tC	0.13	1.35	4.7×10^{13}	21.8
tC^O	0.30	1.35	1.0×10^{14}	28.5
In dsDNA[c]*:*				
tC	0.20	1.40	5.4×10^{13}	23.4
tC^O	0.22	1.40	1.2×10^{14}	27.2

[a] Since the refractive index is a macroscopic property the chosen value of 1.40 is an approximate guess based on the chemical structure of the DNA molecule.

[b] Quantum yield values are for the nucleosides.

[c] Since the quantum yields of tC and tC^O are slightly dependent on neighbouring bases,[61-62] the values used here are averages.

Figure 1. (a) Chemical structure of the tricyclic cytosine analog tC_{nitro} and its base-pairing with guanine. The tricyclic expansion of natural cytosine is highlighted in red. Also shown is the direction of major and minor groove when looking down the long axis of double stranded DNA. (b) Direction of the transition dipole moment, $\vec{\mu}$, associated with the lowest energy electronic transition of tC_{nitro} ($\delta = 27^{o}$). For KtC_{nitro} R = $CH_2COO^-K^+$.

Figure 2. (a) B3LYP/6-31G(d,p) optimized ground state structures of the isolated tC_{nitro} base. Two local energy minima were identified on the PES of tC_{nitro} corresponding to geometries folded along the middle sulphur-nitrogen axis. Left: front view. Right: side view. Bond lengths are given in Ångströms. (b) Frontier KS orbitals of tC_{nitro} optimized at the B3LYP/6-311+G(2d) level.

Figure 3. (a) Isotropic UV-Vis absorption spectrum (full drawn line) and calculated electronic transitions (vertical lines). The absorption spectrum was measured in H_2O at 295 K. Electronic transitions were predicted in the gas phase at the TDDFT B3LYP/6-311+G(2d) level. Note that the calculated excitation energies have been multiplied by a factor 1.08 to facilitate comparison with the UV-Vis absorption spectrum in H_2O. (b) Excitation anisotropy spectrum (red) of the tC_{nitro} nucleoside and reduced linear dichroism spectrum (blue) of the potassium salt of tC_{nitro}. The anisotropy was measured in a propylene glycol glass at 200 K and the linear dichroism was recorded using a stretched PVA film. (c) MCD spectrum of tC_{nitro} nucleoside in a H_2O:methanol mixture (1:2).

Figure 4. (a) Isotropic absorption spectra of tC_{nitro} at various pH values. Arrows indicate increase in pH. pH values used: 8.00, 9.88, 10.22, 10.74, 10.89, 11.13, 11.34, 11.74 and 12.18. (b) Isolated spectra of the protonated (red) and deprotonated form (black) of tC_{nitro} in H_2O obtained from the singular value decomposition (SVD).

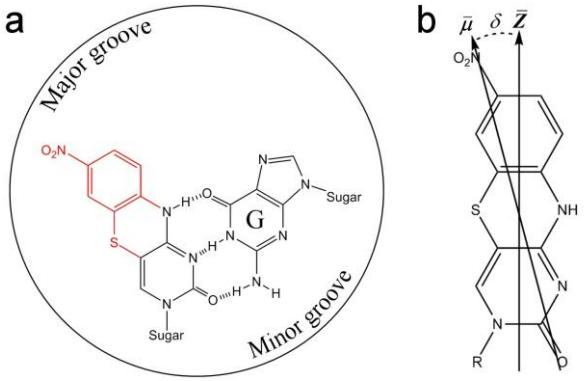

Figure 1.

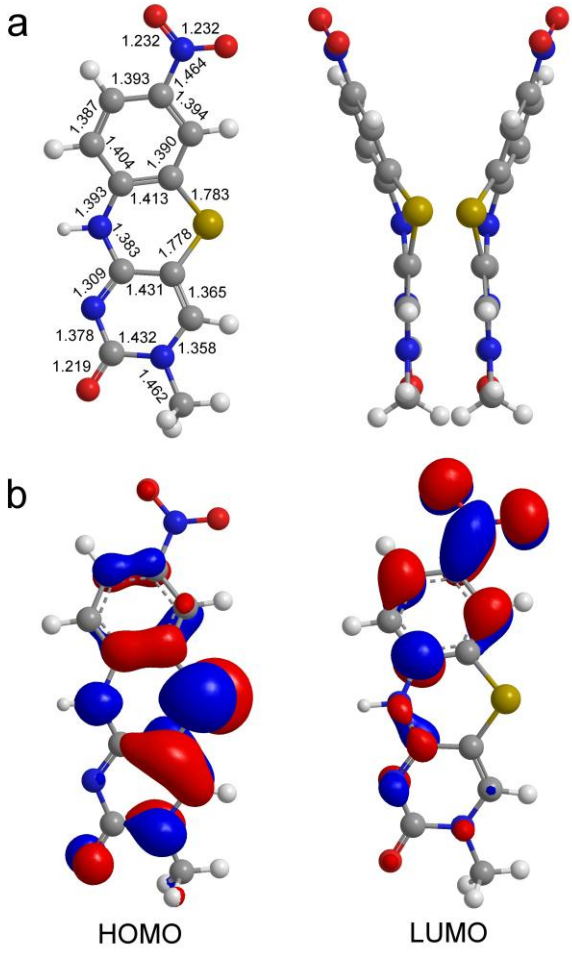

Figure 2.

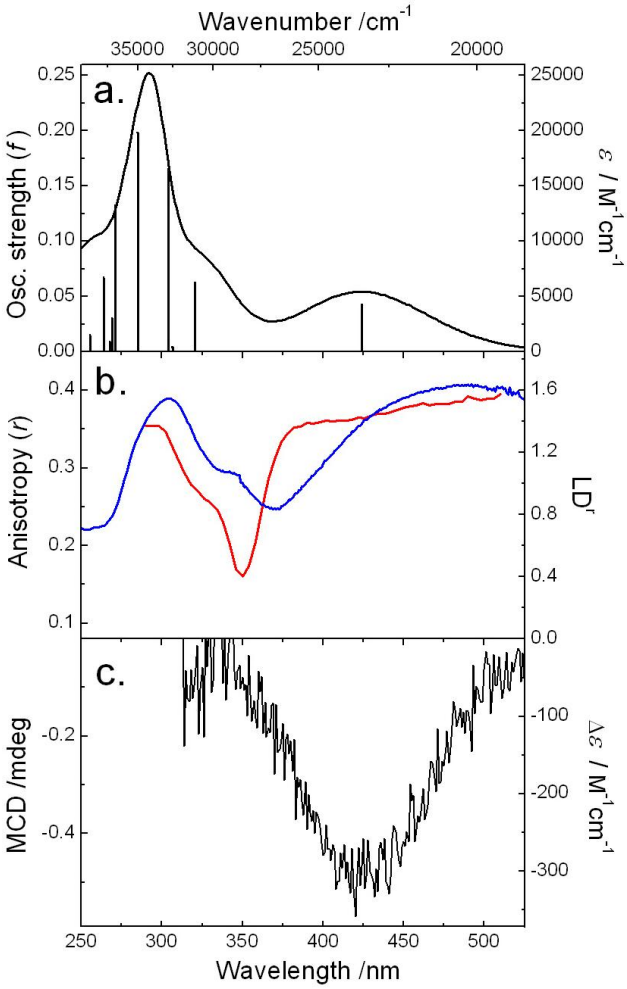
Wavenumber /cm-1
35000
30000
25000
20000
a.
Osc. strength (f)
ε / M-1cm-1
b.
Anisotropy (r)
LDr
c.
MCD /mdeg
Δε / M-1cm-1
Wavelength /nm

Figure 3.

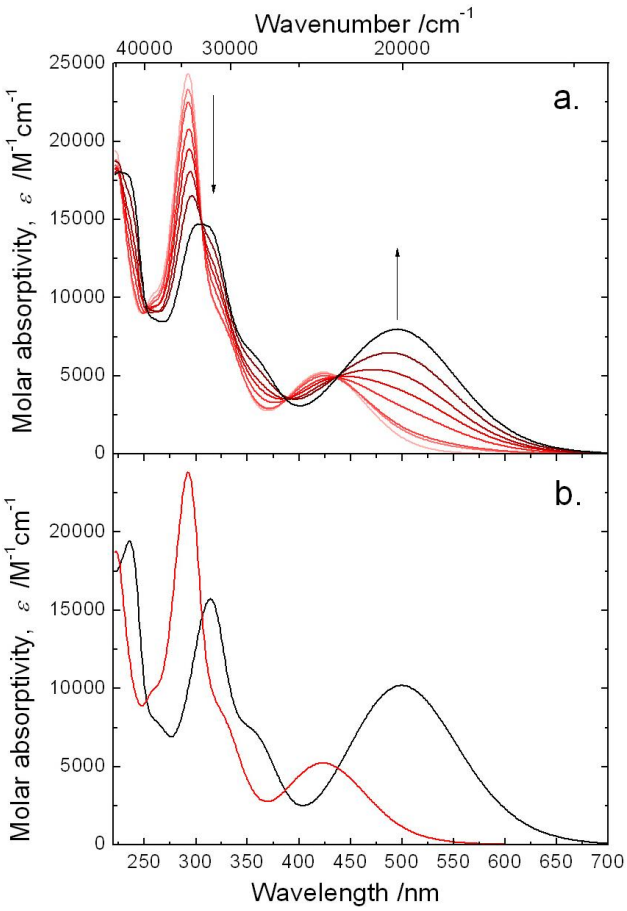
Wavenumber /cm-1
40000
30000
20000
a.
b.
Molar absorptivity, ε /M-1cm-1
25000
20000
15000
10000
5000
0
250
300
350
400
450
500
550
600
650
700
Wavelength /nm

Figure 4.

TOC image: